Distribution Agreement

In presenting this thesis as a partial fulfillment of the requirements for an advanced degree from Emory University, I hereby grant to Emory University and its agents the non-exclusive license to archive, make accessible, and display my thesis in whole or in part in all forms of media, now or hereafter known, including display on the world wide web. I understand that I may select some access restrictions as part of the online submission of this thesis. I retain all ownership rights to the copyright of the thesis. I also retain the right to use in future works (such as articles or books) all or part of this thesis.

Signature

_____ _____

Naifei Zhang Date

Photoelectrochemical Studies on a Triad Electrode for Light-driven Water-splitting

By

Naifei Zhang

Master of Science

Chemistry Department

_____

Craig L. Hill, PhD

Advisor

_____

Tim(Tianquan) Lian, PhD

Committee Member

_____

Cora MacBeth, PhD

Committee Member

_____

Accepted:

Lisa A. Tedesco, Ph.D.

Dean of the James T. Laney School of Graduate Studies

_____

Date

Photoelectrochemical Studies on a Triad Electrode for Light-driven Water-splitting

By

Naifei Zhang

B.S., Wuhan University

China, 2010

Advisor

Craig L. Hill, Ph. D.

An Abstract of
A thesis submitted to the Faculty of the
James T. Laney Graduate School Studies of Emory University
in partial fulfillment of the requirements for the degree of
Master of Science
in Chemistry

2012

Abstract

Photoelectrochemical Studies on a Triad Electrode for Light-driven Water-splitting

By

Naifei Zhang

A photoelectrochemical device is highly desirable for solar to chemical fuel (in our study H_2 is the fuel) conversion. An essential component of such device is the photoanode which absorbs light and catalytically oxidizes water. Here we report a method of fabricating a photoanode by immobilizing a known homogeneous molecular water oxidation catalyst, $[Ru^{IV}_4O_4(OH)_2(H_2O)_4\}(\gamma\text{-}SiW_{10}O_{36})_2]^{10-}$, onto a dye-sensitized nanostructured TiO_2 photoelectrode by electrostatic interaction. The known sensitizers $[Ru(bpy)_2(4,4'\text{-}PO_3H_2bpy)]^{2+}$ (P2) and its modified version $[Ru(5\text{-crown-phen})_2(dpb)]^{2+}$, dpb =4,4'-diphosphonic acid 2,2'bipyridine (C2P2) were both used. The polyoxometalate catalyst with different cations (inorganic and organic cations) was used. The effect of sensitizers and catalysts on photoelectrochemical properties were compared and discussed. An enhanced photocurrent is observed with the triad photoanode FTO/TiO_2/P2/THpA-Ru_4POM with an applied bias of 500mV and FTO/TiO_2/C2P2/THpA-Ru_4POM with no external bias. The bias-dependent behaviors of the photocurrent are in good agreement with calculated frontier orbitals.

Photoelectrochemical Studies on a Triad Electrode for Light-driven Water-splitting

By

Naifei Zhang

B.S., Wuhan University

China, 2010

Advisor

Craig L. Hill, Ph. D.

A thesis submitted to the Faculty of the
James T. Laney Graduate School Studies of Emory University
In partial fulfillment of the requirements for the degree of
Master of Science
in Chemistry

2012

Table of Contents

List of Abbreviations

Abs	Absorbance
C2P2	$[Ru(5\text{-crown-phen})_2(dpb)]^{2+}$ (dpb =4,4'-diphosphonic acid 2,2'bipyridine)
FTO	Fluorine doped Tin Oxide
MLCT	Metal-to-ligand charge transfer
P2	$Ru(bpy)_2(4,4'\text{-}PO_3H_2bpy)Cl_2$
PECs	Photoelectrochemical cells
POM	Polyoxometalate
PV	Photovoltaic
Ru_4POM	$[Ru^{IV}{}_4O_4(OH)_2(H_2O)_4\}(\gamma\text{-}SiW_{10}O_{36})_2]^{10-}$
THpA	Tetraheptyl ammonium
UV-Vis	Ultraviolet-Visible
WOC	Water-oxidation catalyst
WRC	Water-reduction catalyst

List of Figures

Chapter 1

Chapter 2

Chapter 3

List of Schemes

Chapter 1

Chapter 1:

Introduction

1.1 General Introduction

The availability of energy determines our civilization's survival on this planet[1]. We have been relying heavily on fossil fuels for the past century but the shortcomings of this practice are obvious: the efficiency of combustion is low while the waste gas released from the burning process raises environmental issues such as photochemical smog, acid rains and global warming. In addition, the detected exploitable fossil fuel reserves in the world can only last for another 150 years at our current consumption rate[2]. This is threatening unless alternative energy resources that are renewable, globally accessible and environmentally friendly can be developed in the near future [1, 3-5].

Solar energy is clearly the ultimate solution. The earth receives about 1,366 watts of direct solar radiation per square meter[6], an incredible amount of energy that is far more than all other renewable energy resources (wind power, geothermal, biomass, hydroelectric, etc) combined. It has been estimated that the energy of solar radiation in a single hour can power the whole world for an entire year[7]. Another surprising solar energy fact is that 99.9% of currently goes to waste. Green plants have been harvesting sunlight and utilizing this energy to convert water and carbon dioxide to oxygen and sugar via a process known as natural photosynthesis. But the efficiency is typically below 1%[8].

Thus the real challenge for scientists in utilizing solar energy is therefore a more efficient and fast energy conversion system. There are mainly 3 ways to convert solar

energy: thermal conversion (to heat), photovoltaic conversion (to electricity) and photochemical conversion (to chemical fuels) [9-11].

Thermal conversion is the easiest but it suffers from the difficulties of heat storage, transportation and utilization. Compared to photochemical conversion, its more heavily studied cousin, photovoltaic conversion of solar energy, has taken a step further ever since the discovery of semiconductor materials. With a good solid-state photovoltaic device, one can easily convert sunlight to electricity as long as the material's band gap reasonably matches the solar spectrum[12, 13]. Great effort has been made to maximize the conversion efficiency of photovoltaic devices (so far 49% has been reported to be achievable for silicon[12]). However, photovoltaic devices are subjected to high production costs and electricity is problematical to store efficiently and in large quantities.

1.2 Light-Driven Water-Splitting

Chemists have been trying to capture solar energy and store it in the form of chemical bonds. One of the most studied reactions is light-driven water-splitting which produces oxygen and hydrogen[14], the latter being a clean and renewable fuel that only produces water during combustion. The stability of water molecules makes conventional electrolysis a notoriously energy-intensive process. By using sunlight as the driving force for the reaction, scientists are able to develop a system that splits water with minimum input of electricity[15].

$$H_2O + h\nu \rightarrow H_2 + \tfrac{1}{2} O_2 \qquad \text{eq. 1}$$

$$2H_2O \rightarrow 4H^+ + O_2 + 4e^- \qquad \text{eq. 2}$$

$$2H^+ + 2e^- \rightarrow 2H_2 \qquad \text{eq. 3}$$

However, the seemingly straightforward reaction in eq.1 is not simple in mechanism or application. The light-assisted water-splitting process can be broken down into 4 key components: the capture of solar energy by a photosensitizing device; the reduction of water into protons (eq. 2); the coupling of these protons into hydrogen gas (eq. 3); and the oxidation of water into oxygen gas (eq. 2)[16, 17]. To promote charge-hole separation, semiconductors are often as the photosensitizer.

For each half reaction, extensive research has been conducted and is ongoing. Electrochemical methods are frequently involved since they can probe the reaction by directly injecting or draining electrons. This requires the use of a standard electrochemical cell and electrodes, on the surface of which the half reactions take place. The reason to study half reactions on electrodes separately is that the research goal and methods are simplified and the products of the reaction----hydrogen and oxygen----are spatially well separated so that they can be collected without danger of explosion or recombination which lowers the yields. A greater implication of this study is the possibility of a cell device that decomposes water when immersed in water.

It should be noted that the water-oxidation reaction on the electrode illustrated in eq. 2 is frequently the rate-determining step and it is sluggish even with the best catalysts

reported so far compared to the hydrogen reduction reaction. Water-oxidation is usually slow and inefficient in part because it's a four-electron process involving the coupling of electron transfer with proton transfer. For most systems (catalysts), it is still a matter of debate as to how electrons are transferred and how the oxygen-oxygen bond is formed, making catalytic water-oxidation research a very engaging and active area.

1.3 Photoelectrochemical Solar Cells (PECs)

Photoelectrochemical cells, or PECs, are devices that generate fuel from sunlight via chemistry-involving processes, while photovoltaic cells, or PV cells, in contrast generate electricity (current at a particular potential). A major difference in device design is that the solid-state junction in PV cells is completely replaced by a semiconducting material interfacing with an electrolyte[18]. Historically, Becquerel in 1839 first discovered "photoelectric" effect on an electrode immersed in a conductive liquid. This was the start of photoelectrochemical research. Lewis et al. developed regenerative (electricity producing) photoelectrochemical cells of notable efficiency in the 1980's. Michael Grätzel from EFPL in Lausanne, Switzerland, reported efficient regenerative PECs based on dye-sensitization in 1991. There are typically 2 types of PECs, one is the dye-sensitized solar cell (DSSC) led by Grätzel's research. The other is a photoelectrosynthetic cell in which a chemical reaction is driven by solar energy and chemical fuels are created. An example of such a PEC is one for water splitting, eq 1. Such cells are partly inspired by natural photosynthesis and this area in

commonly referred to as artificial photosynthesis (AP). The "Hydrogen Economy" has been and is a driving force in the development of low-cost and efficient PECs.

PECs have gained unprecedented attention and challenged the dominance of PV devices for 2 reasons: they store solar energy as energy-dense chemical fuels and they reduce the cost of materials and fabrication substantially.

A typical water-splitting PEC device consists of dye-sensitized semiconductor photoanode coated with high-efficient water oxidation catalyst, a hydrogen-producing cathode (usually platinum) and electrolyte, as illustrated in Scheme 1.1. Upon radiation, photoexcited electrons that are immediately injected into the conduction band of TiO_2 pass through an external circuit to reduce protons to hydrogen at the counter electrode while the holes left in the valence band of TiO_2 are consumed by water to produce oxygen. Schematic energy diagram in Scheme 1.2 shows the flow of electrons. A photocatalyst for water oxidation and a catalyst for proton reduction are usually used to accelerate the chemical reactions, thus minimizing the charge-hole recombination in the semiconducting material and increasing the overall PEC efficiency.

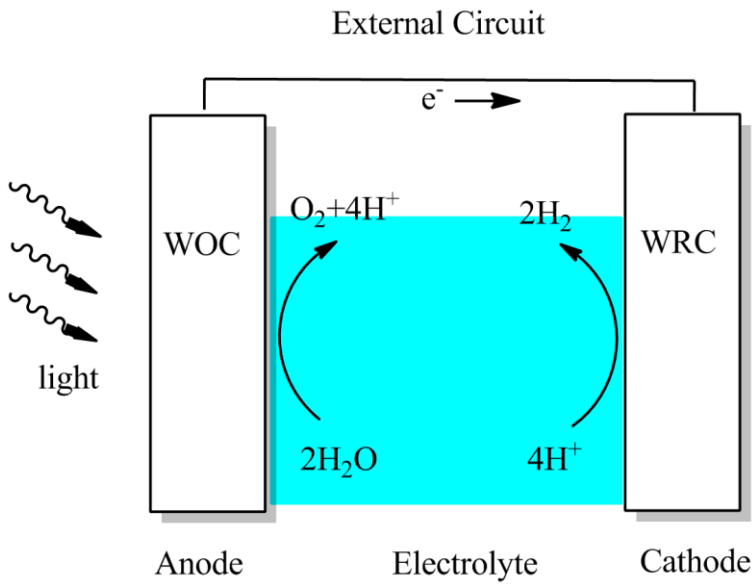

Scheme 1.1 Proposed schematic of a photoelectrochemical cell for water splitting.

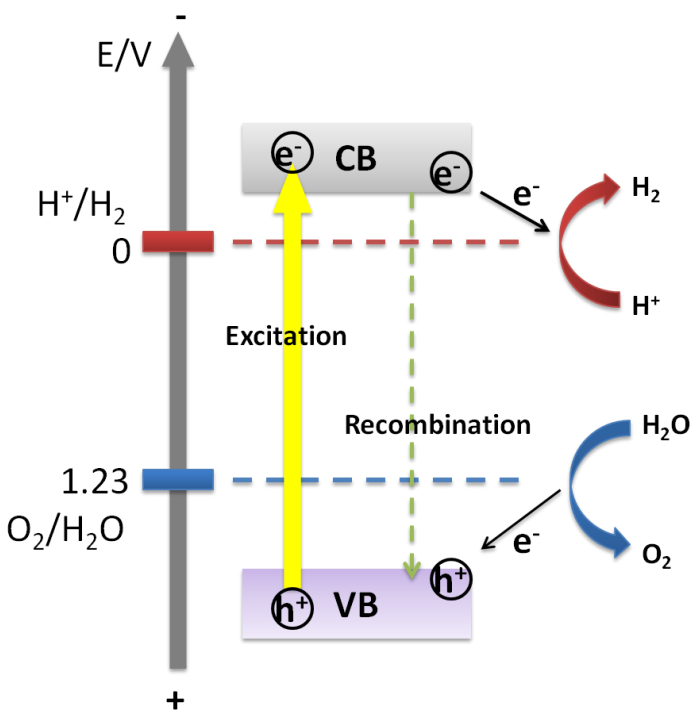

Scheme 1.2 Energy diagram of photocatalytic water splitting[19]

1.4 Sensitizers

Sensitization[20] is very important for PECs since TiO_2, a popular semiconductor material because of its low cost, great stability and non-toxicity, has a band gap of 3.2eV. This high-energy band gap only facilitates absorption of a small region of solar radiation; most visible light in the solar spectrum is unused. Sensitization methods generally include doping[9, 21-23] and dye-sensitization[24, 25]. The former is used and studied by solid-state physicists rather than chemists.

Sensitizers or light-harvesting components are molecules in which electron excitation occurs upon illumination, Many intensely-colored d^6 transition metal complexes, and in particular Ru(II) polypyridine complexes, are useful photosensitizers for electron transfer and energy transfer processes[26, 27]. The widely used tris(2,2′-bipyridine)ruthenium(II) complex $[Ru(bpy)_3]^{2+}$ (bpy = 2,2′-bipyridine), can be modified by the introduction of electron-donating groups (EDG) and electron-withdrawing groups (EWG) in the 4 and 4′ positions of 2,2′-bipyridine[28-32]. The properties of the photosensitizers, such as absorption spectrum, lifetime of the excited state, quantum yield and redox potentials, which are dramatically affected by the functional groups in ligands, are thus tunable through synthesis. For example, when the EWG –COOH is introduced to $[Ru(bpy)_3]^{2+}$, the p* level of bpy ligand is lowered and thus MLCT transition is red-shifted. The MLCT state is better stabilized in $[Ru(dcbpy)_3]^{2+}$ compared to the parent complex, resulting in an increased lifetime, a finding that has been confirmed by Seenivasan and coworkers[29].

Another merit of functional groups is that they enable binding or “anchoring” of the dye molecule to the surface of solid substrate[33, 34] such as TiO_2. In this way,

sensitizers are tightly bound to the solid surface via chemical bonds and are less likely to fall off. Anchoring groups such as $–PO_3H_2$ and –COOH are commonly used because they easily form metal-oxygen-phosphorus and metal-oxygen-carbon bonds with TiO_2.

In this work, compounds $Ru(bpy)_2(4,4'\text{-}PO_3H_2bpy)Cl_2$ (P2 for short) and P2-functionalized by crown ether (C2P2 for short) are used as sensitizers. They were synthesized and characterized by Dr. John Fielden in Professor Craig Hill's group. P2 has been extensively used as a sensitizer by research groups[35] studying photoelectrochemical devices based on dye-sensitized TiO_2 electrodes and it has two phosphonates as anchoring groups. C2P2 was first reported by Dr. Fielden. C2P2 has higher extinction coefficients than P2 and its ether groups are able to capture and bind cations such as Na^+ making them more strongly attracted to anions. (The WOCs in this work are highly charged polyanions). The UV-Vis spectra of the two sensitizers are shown in Figure 1.3. The absorption peak data and oxidation potentials obtained from electrochemical measurements are summarized in Table 1.1.

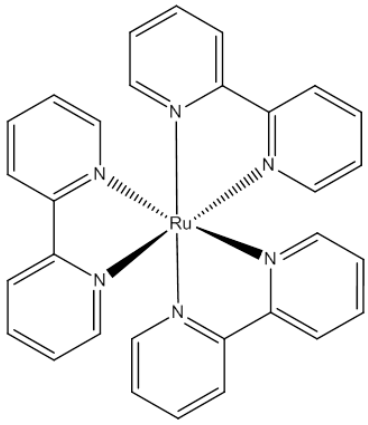

Figure 1.1 Molecular structure of $[Ru(bpy)_3]^{2+}$

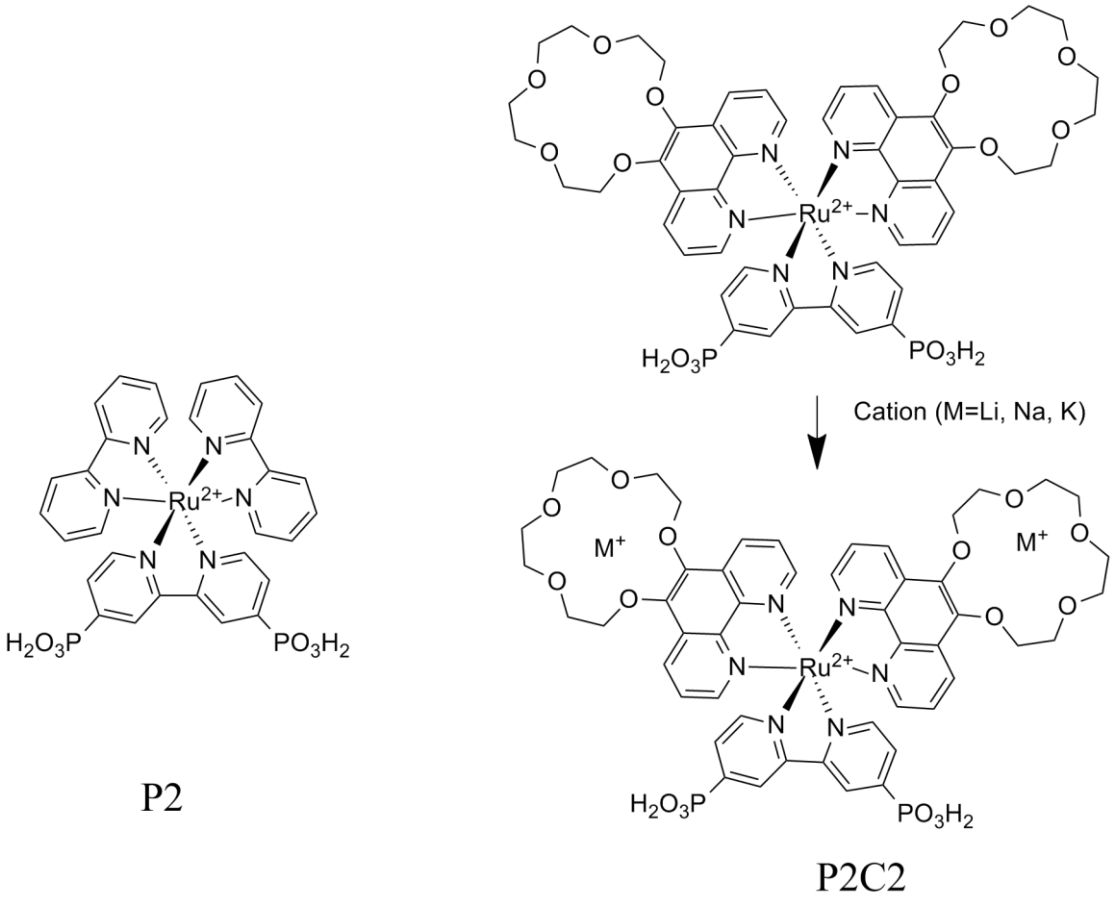

Figure 1.2 Molecular structures of P2 and C2P2.

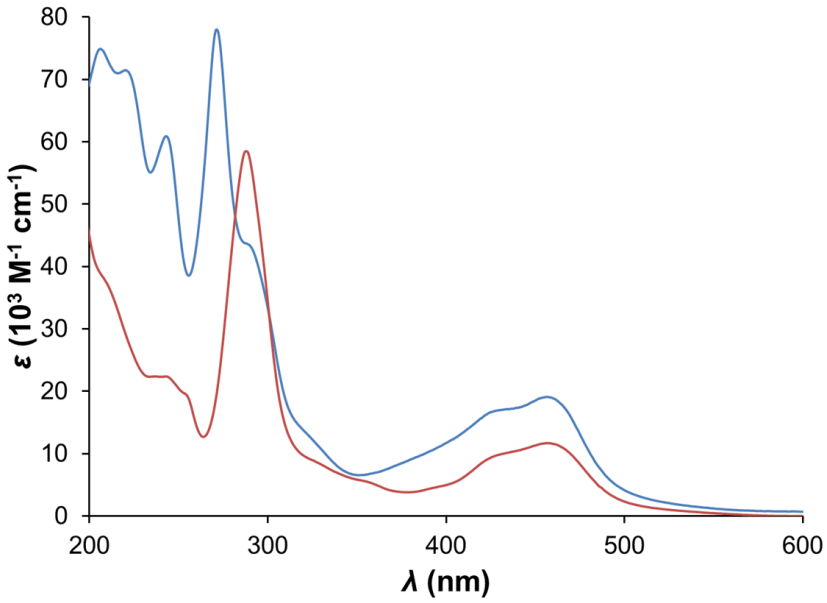

Figure 1.3 UV-Vis Spectra of P2 (red) and C2P2 (blue).

	λ_{MLCT} (nm)	ε_{MLCT} (M^{-1} cm^{-1})	$E_{1/2}$, $Ru^{2+/3+}$ (V, vs SCE)
P2	456	11700	1.39
C2P2	457	19100	1.40

Table 1.1 Absorption and oxidation potential data of P2 and C2P2.

1.5 POM WOCs

Developing a viable water-oxidation catalyst (WOC) has remained a challenge for years even though the community now does have some catalysts that exhibit high efficiency and stability [36-41]. An effective water-oxidation catalyst must be: 1) stable to air, water and heat (oxidative, hydrolytic, and thermal stability); 2) chemically robust; 3) low cost. There are many research groups working on heterogeneous [15, 42-52] and homogeneous [53-65] WOCs. Heterogeneous WOCs are generally of lower in cost, more durable, and more easily immobilized onto electrodes; however, they harder to study and thus to optimize. The mechanism of their catalytic activity for water oxidation remains largely unclear. In addition, heterogeneous WOCs tend to aggregate into low-surface-area inactive clusters over time[66]. Homogeneous WOCs, though not readily applicable for devices, provide a model for us to investigate and understand mechanisms and are easier to improve because they can be probed by many instrumental and computational methods. Many homogeneous WOCs however, have organic ligands that are subjected to oxidative degradation, processes which are frequently accelerated when irradiated[67, 68]. To develop carbon-free homogeneous WOCs is a key to stable and durable WOCs.

Polyoxometalate (POM) research is a dynamic field of study at the interface of inorganic chemistry, materials and catalysis [40, 41, 69, 70]. POMs are heteropolyoxoanions containing transition metals in their highest oxidation state bridged by oxygen atoms. These transition metals are commonly tungsten or

molybdenum, and less commonly vanadium, niobium or tantalum. These inorganic clusters are highly anionic with charges up to 10- or higher.

POMs have recently emerged as a new class of molecular catalysts for green organic oxidation processes in part because their compositions can be extensively controlled, they form well defined structures, and they exhibit redox-leveling properties in multi-electron transfer processes. In addition, they are low in toxicity and highly durable. The Hill group at Emory University has developed a family of POM WOCs, and one of these is the Co_4POM that combines stability, selectivity with an exceptionally high rate for oxygen evolution while being composed only of earth-abundant-elements [40]. The first all-inorganic molecular and soluble WOC was $[\{Ru^{IV}_4O_4(OH)_2(H_2O)_4\}(\gamma\text{-}SiW_{10}O_{36})_2]^{10-}$ (Ru_4POM for short), whose X-ray structure is shown in Figure 1.4[40]. This POM can catalyze the visible-light-driven oxidation of water to oxygen in a buffered system (pH~7.2) containing the photosensitizer $[Ru(bpy)_3]^{2+}$ and the sacrificial electron acceptor $Na_2S_2O_8$. At Ru_4POM concentrations as low as 5.0μM, decent chemical yields and quantum yields (up to 30% after optimization) are observed[71]. The proposed mechanism is depicted in the scheme below.

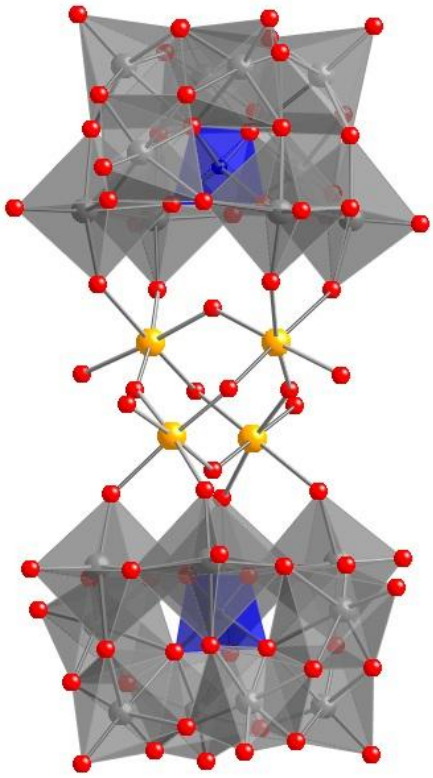

Figure 1.4 X-ray crystal structure of the polyanion Ru_4POM (adapted from published paper[41]) showing the Ru_4O_4 core sandwiched between two tetra-dentate stabilizing polytungstate ligands. The WO_6 octahedra and central SiO_4 tetrahedra in the polytungstate ligands are gray and navy blue, respectively. Ru: yellow. O: red. W: gray. Si: blue.

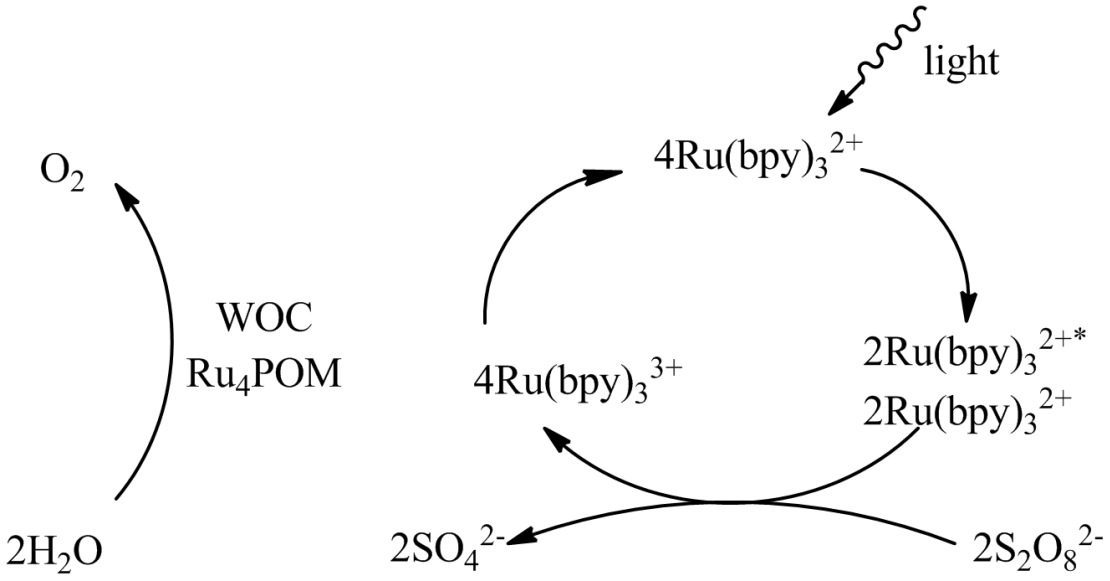

Scheme 1.3 Scheme for Ru_4POM catalyzed oxidation of water to oxygen in a buffered system with photosensitizer and sacrificial electron acceptor.

Chapter 2:

Experimental Section: Preparation of Electrodes, Investigation of Stability and Photoelectrochemical Performance

The photoelectrodes were prepared by immobilizing the POM WOCs on nano-structured TiO_2 electrodes. Synthesis of TiO_2 colloid was based on published procedures. The photosensitizers (also commonly referred to as "sensitizers") in this work were used as received from Dr. John Fielden. The water-soluble water-oxidation catalyst, the inorganic salt of $[Ru_4O_4(OH)_2(H_2O)_4(SiW_{10}O_{36})_2]^{10-}$ was used as received from Dr. Craig Hill's group. The modified version of this catalyst, the organic salt of $[Ru_4O_4(OH)_2(H_2O)_4(SiW_{10}O_{36})_2]^{10-}$, was synthesized and purified based on published method[72]. UV-Vis spectroscopy was used to examine the loading of dye molecules and the stability of the electrodes. Photoelectrochemical measurements were conducted to investigate the light-assisted catalytic water oxidation performance of the electrodes.

2.1 Materials and Preparation

2.1.1. Preparation of TiO_2 Colloid and Film

TiO_2 nanocrystalline thin films were prepared by a sol-gel method followed by growth under hydrothermal conditions, a procedure similar to that used by Zaban[73]. Briefly, 250 mL of water and 80 mL of acetic acid were mixed in a 1000 mL round bottom flask in ice bath. A mixture of 10 mL of 2-propanol and 37 mL of titanium (IV) isopropoxide (Aldrich, 97%) was then dropped slowly into the acetic acid solution within over a period of 30 min with vigorous stirring. N_2 was continuously bubbled through the preparation vessel simultaneous with stirring. After stirring overnight, the transparent colloid was transferred to a 1000 ml beaker and heated in a 80 °C hot water bath for 3-4 h with vigorous stirring. The resulting gel was autoclaved at 230 °C for 12 h and then cooled down to room temperature slowly. About 20 drops of TritonX-100 (Aldrich) was added to 10 mL of the colloid and the solution was stirring for at least one day. TiO_2 colloids are sensitive to light so they were kept in the dark when not stirred.

To make films, cleaned FTO glass was put on the bench with the conductive side face up and they were anchored by Scotch® tape. The adhesive tape serves as a spacer which controls the thickness of the films [74]. One or two drops of the TiO_2 colloid were dispersed on the conductive surface, spread by a glass rod and then dried in air. Fifteen minutes later the films were baked at 400℃ in oven for 1 h, resulting in almost transparent films.

2.1.2 Sensitizers Used in This Work

The sensitizers used in this work are $Ru(bpy)_2(4,4'\text{-}PO_3H_2bpy)Cl_2$ (P2 for short) and P2 functionalized by crown ether rings (C2P2 for short). Both sensitizers were synthesized and purified by John Fielden and both have two phosphonate groups facilitating binding to the TiO_2 surface, i.e. making M-O-P bonds.

2.1.3 WOCs Used in This Work

Inorganic salt of Ru_4POM

The ruthenium-substituted polyoxometalate, $[Ru_4O_4(OH)_2(H_2O)_4(SiW_{10}O_{36})_2]^{10-}$ (Ru_4POM), was synthesized and purified by the Hill Group using the literature procedure[71]. Ru_4POM is highly soluble in water if the counterions are potassium, rubidium or a mixture of these.

Organic salt of Ru_4POM

The tetraheptyl ammonium (THpA) salt of Ru_4POM, a hydrophobic salt of the highly soluble original compound, was synthesized according to reported methods[37]. Previously, Pope and coworkers[75] studied the preparation of transition-metal-substituted POMs in anhydrous non-polar solvents and reported that the THpA cations associate with the metal substituted POMs and extract them from aqueous solution to highly non-polar organic solvents such as toluene.

2.2 Electrode Assembly

2.2.1 Dyad Electrode

Sensitizers were weighed and dissolved in ethanol to make 1mg/1mL dye-ethanol solutions. P2-ethanol is a clear reddish-orange solution while C2P2-ethanol is an orange-yellowish solution. Ultrasonication helps the dye to dissolve in ethanol. Dye solutions should always protected from the light by covering the glass containers with tin foil.

Binding of the dyes to the nanoporous TiO_2 films was accomplished by soaking the films in a dye solution. After this binding (immobilization) process, the film was rinsed with distilled water to wash off non-chemically adsorbed dye molecules. To ensure complete removal of these physisorbed extra dye molecules, the dye-treated films were further washed in distilled water for another 2 hr. After dying in air at room temperature, the yellow colored films obtained from this procedure were referred to as "sensitized films" or "dyad electrodes".

2.2.2 Triad Electrode

Functionalized triad electrodes were made by further soaking of the sensitized films in a solution of the catalyst.

Water-soluble salts of POM were weighed and dissolved in distilled water to make 100 μM solutions. Organic-soluble salts were dissolved in toluene to make 100μM

solutions. Dyad films were soaked in POM solutions for up to 30 min, then removed and dried in air at room temperature. Association (binding) of the POMs to the dye-modified electrode surfaces either by electrostatic adsorption or chemisorption should be fairly rapid.

The organic layer provides a hydrophobic environment that prevents detachment of the sensitizers from the TiO_2 surface. All data given and discussed below were based on electrodes modified by THpA-Ru_4POM. Dyad electrodes with a structurally identical redox-inactive Zn_4POM were compared with the triads containing the WOC.

2.3 UV-Vis Spectroscopic Measurements

Loading of dyes on the TiO_2 films was measured using an Agilent UV-Vis Spectrometer. The stability of the electrodes is closely related to the rate and percentage of dye loss from the TiO_2 surface.

There were two ways to take a UV-Vis spectrum of the electrode. In one way, the electrode was first assembled in a photoelectrochemical cell (Figure 2.1) and electrolyte was filled in to just immerse the electrode. The whole cell was put in the spectrometer for a spectrum to be taken. This spectrum reflects the absorbance of the entire system----electrode and electrolyte. In the other, the electrode was taken out from the cell and dried in air, then put in the spectrometer for a spectrum to be taken. This spectrum reflects the absorbance of electrode alone.

In the data shown in Chapter 3, how the spectra were taken was noted as “in solution” or “dry films”. Also it showed whether a PEC measurement had been conducted, with

(light reaction) or without illumination (dark reaction) before the spectrum was taken. Each PEC measurement usually took 5 min.

The percentage of dye loss was calculated from the decrease in absorption bands in the UV-visible spectra.

2.4 Photoelectrochemical Measurements

Photoelectrochemical experiments were conducted with a BASi potentiostat by using the standard three-electrode configuration in a one-compartment cell. The buffering electrolyte was a solution of 30 mM Na_2SiF_6 (adjusted to pH 5.75 with $NaHCO_3$) based on a similar study by Mallouk[15]. The buffer was made by dissolving 0.595g Na_2SiF_6 and 0.447mg $NaHCO_3$ in 33mL and 67mL water respectively, mixing the solution and ultrasonicating. A small amount of $NaHCO_3$ was added to 100 mL of the solution to adjust the pH to 5.75. The reference electrode was Ag/AgCl, which is 0.250V more positive than RHE. A Pt wire was used as the counter electrode.

Single-potential time-based and cyclic voltammetry techniques were both used.

For single-potential time-based experiment, the applied bias was denoted in the data.

For cyclic voltammetry, the scanning rate was always 50mV/s and the scanning range was 0~1000mV.

Illumination was provided by a Xenon lamp (C2577 from Hamamatsu). Two filters were used after the beam had been aligned. The aligned beam was between 430 nm to 470 nm in wavelength and ~1.3 cm in diameter, a slightly larger area than the coated

area (ca. 1 cm^2) of the FTO electrode itself. The measured illumination intensity was around 17 mW/cm^{-2}. See Figure 2.1.

Illumination was used in “light reactions” but not in “dark reactions”, as denoted in the data in the next chapter.

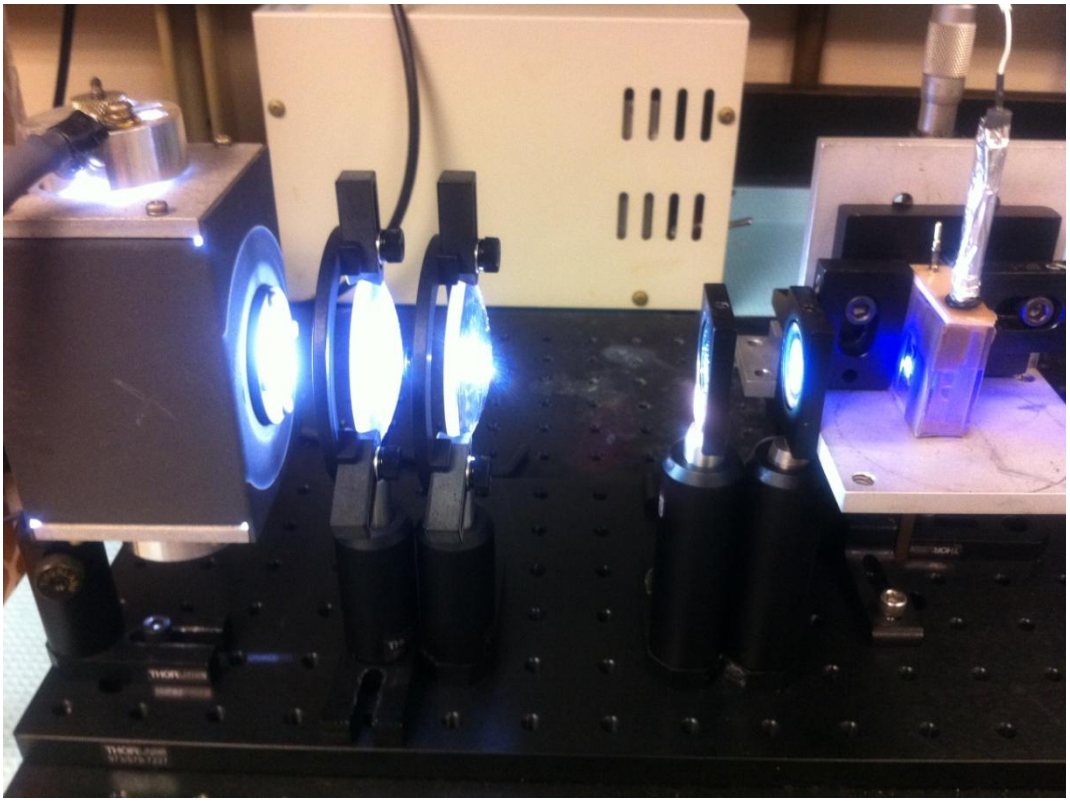

Figure 2.1 Photograph of the experimental setup for the photoelectrochemical measurements

Chapter 3:

Results and Discussion

The results on electrodes with different sensitizers are reported in two parts: TiO_2/P2/WOC and TiO_2/C2P2/WOC. This is because the choice of sensitzers in this triad system has a huge effect on the photocurrent, which exhibits bias-dependent character. In each part, the results and discussion on stability is followed by those on photocurrent. The stability of C2P2 is similar to that of P2 based on the time-dependence of the electronic absorption spectra, and therefore the detailed time-dependent spectra of triad electrode with C2P2 are not shown. Only the percentages of dye lost in all systems are compared. The single-potential time-based technique is the most direct way of evaluating photocurrent while cyclic voltammetry gives a better overview of catalytic water oxidation activity. In the C2P2-based system, the CV data are not shown to avoid redundancy in exhibiting the photocurrent results. Only current-time (i-t) data under different external bias are shown because the C2P2-based system exhibits more interesting bias-dependent character.

3.1 Electrode with P2 as Sensitizer

3.1.1 UV-Vis spectra and Stability

The dyes are known to bind to TiO_2 surface via phosphonate groups[31]. It is observed that dyads in either borate or phosphate buffers are not stable at all: the yellow colored film becomes almost colorless in less than 5 min after immersion in the electrolyte. It has been concluded that phosphate and borate compete with the phosphonate-substituted Ru dye, and these buffer nucleophiles (in great molar excess) eventually result in displacement of the Ru-based dyes from the TiO_2 surface. The dyads are quite stable in unbuffered solutions such as distilled water or 0.2M aqueous NaCl.

However, water oxidation catalysis has to be done in buffered solutions and we chose the Na_2SiF_6-$NaHCO_3$ buffer system which proved to be less reactive (less prone to displacing the surface-immobilized dyes). The concentration of dyes bound to the TiO_2 decreased by 30~40% within the first 5 min after immersion of the dyads. A bound-versus-solution dye equilibrium was soon established and dye loss was much slower in the next hour when the photoelectrochemical measurements were being conducted.

Figures 3.1 and 3.2, respectively, demonstrate the stability of dyad and triad electrodes with the immobilized THpA salt of Ru_4POM. Data from the triad with water-soluble and TBA salts of Ru_4POM are not shown since they showed poorer stability and far less noticeable photocurrent enhancement.

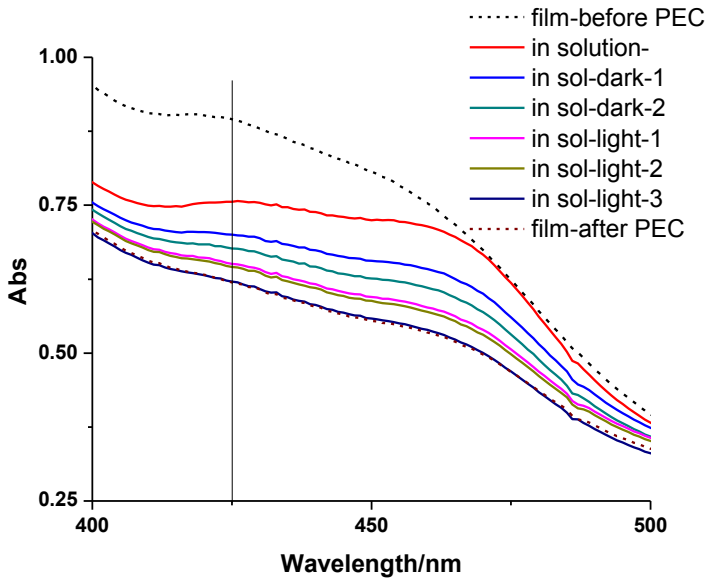

Figure 3.1 UV-Vis spectra of P2-based dyad electrode showing stability of dyad electrode. Changes in the UV-Vis spectra of the electrode while immersed in buffer for PEC measurement (solid lines, from top to bottom) are shown. Changes in the UV-Vis spectra of the dry dyad electrode are shown as short dashed lines. Each PEC measurement here referred to a cyclic voltammetry of about 10 segments, 5 min.

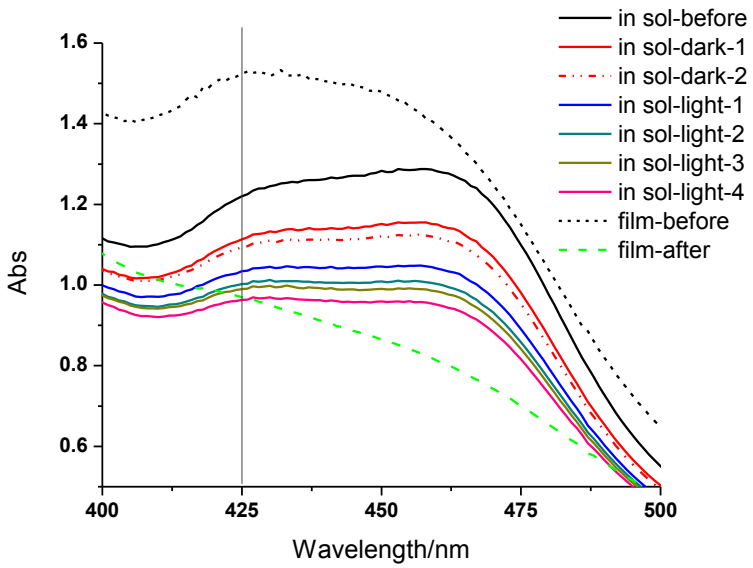

Figure 3.2 UV-Vis spectra of P2-based triad electrode showing stability of triad electrode. Changes in UV-Vis spectra of electrode while immersed in buffer for PEC measurement (solid lines, from top to bottom) are shown. Changes in UV-Vis spectra of the dry triad electrode with THpA-Ru_4POM (as short dashed lines) are shown.

3.1.2 Photoelectrochemical Measurements

Single-potential time-based technique

For the P2 dye, electron injection from the photosentizer to the TiO_2 and charge transfer from the catalyst molecule THpA-Ru_4POM to the dye molecule have been observed with an applied bias of 500 mV.

Figure 3.3 demonstrates the transient short-circuit photocurrent generated upon the on–off cycle illumination of the TiO_2–P2/Ru_4POM anode (red line). Neither the anode with the dye but without the WOC (catalyst; black line) nor the electrode with the dye and a redox-inactive THpA-Zn_4POM (blue line) generates a significant current (black line). Clearly almost no electrons pass through the external circuit in the presence of P2 but in the absence of catalyst. Upon illumination, the photosensitizers are excited and inject one electron into the conduction band of TiO_2. The one-electron-oxidized sensitizer PS^+ then removes an electron from the POM, regenerating itself while oxidizing the POM. The immobilized POM, after multiple oxidations, subsequently oxidizes water to oxygen. The electron in TiO_2 passes through the external circuit and recombines with a proton to produce hydrogen at the cathode.

Some further points on the shape of the time-current curve: when the light is turned on, injection of electron from sensitizer to TiO_2 is rapid and relaxation of the excited dye molecules is immediate creating a sharp spike. The current then starts to drop slowly eventually leading to a relatively stable photocurrent. When the light is blocked, the system becomes a pure photovoltaic device and generates a current of opposite sign, and a smaller spike is seen.

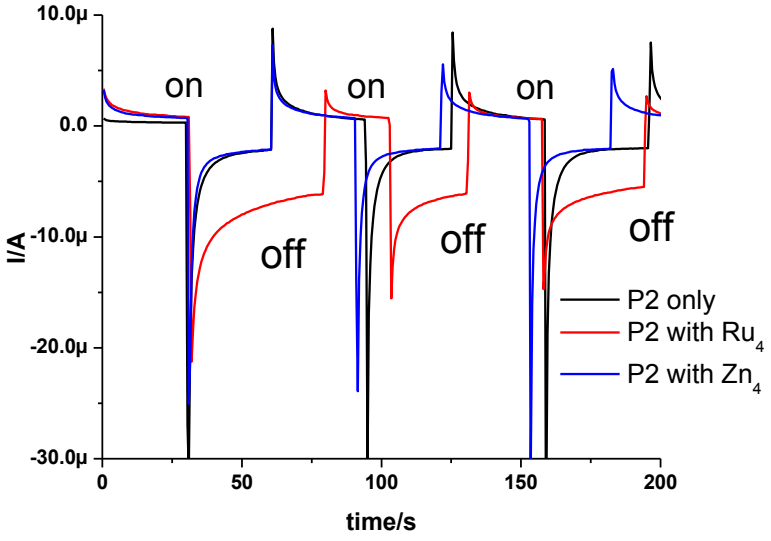

Figure 3.3 Single-potential time-based results for dyad (black), triad with THpA-Ru_4POM (red) and the control triad with THpA-Zn_4POM (blue) at an applied bias of 500 mV.

Cyclic Voltammetry

Data from cyclic voltammmetry provide additional evidence of enhanced photocurrent from the triad with Ru_4POM compared to the control electrodes. As shown in Figure 3.4, for the dyad electrode and triad electrode with Zn_4POM, the dark currents and light currents are similar. In contrast, a photocurrent of about 20 μA (difference between solid line and dashed line) is observed for the triad electrode with Ru_4POM.

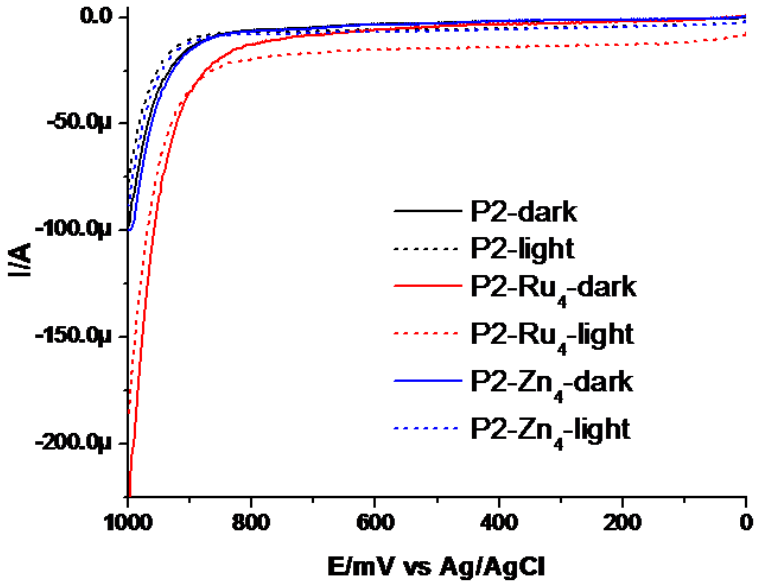

Figure 3.4 Cyclic voltammetry of the dyad (black), the triad with THpA-Ru_4POM (red) and control triad with THpA-Zn_4POM (blue).

One limitation of these experiments is the lack of characterization of the POMs on the electrode surface. Presumably, only an approximate monolayer of POM molecules is bound to the surface. Monolayers typically do not contain enough sample to be detectable by UV-Vis spectroscopy. Indeed in our cases in this study here no characteristic absorbance from the POM under neutral conditions is evident. In addition, ATR-IR, in the absence of enhancement mechanisms, is not sensitive enough either for detection of a monolayer of absorbed molecules. Two methods for characterizing electrode-surface-immobilized POMs in future studies include XPS (X-ray photoelectron spectroscopy) and XFS (X-ray fluorescence spectroscopy). We are pursuing the use of these techniques in collaboration with other teams at U.C. Berkeley and elsewhere because they are not available presently at Emory University. It has been shown that POMs absorb over the entire UV-Vis wavelength range. Thus the UV-Vis spectra can be used to roughly distinguish the dyad and triad electrodes but not to distinguish two triad electrodes with different THpA-POMs . Figure 3.5 shows the UV-Vis spectra of dyad electrodes, the triad electrode with THpA-Ru_4POM and the triad electrode with THpA-Zn_4POM. Three electrodes were made from three dyad films with the same dye loading (black line, red line and blue line). Two of them were further soaked in POM solutions to make the triad electrodes. After this process, their UV-Vis absorbance over the entire wavelength range increased (cyanine-green and magenta lines), which is probably consistent with electrode-surface-immobilized POM molecules. Scattering in the organic layer could also partly explain the spectral change.

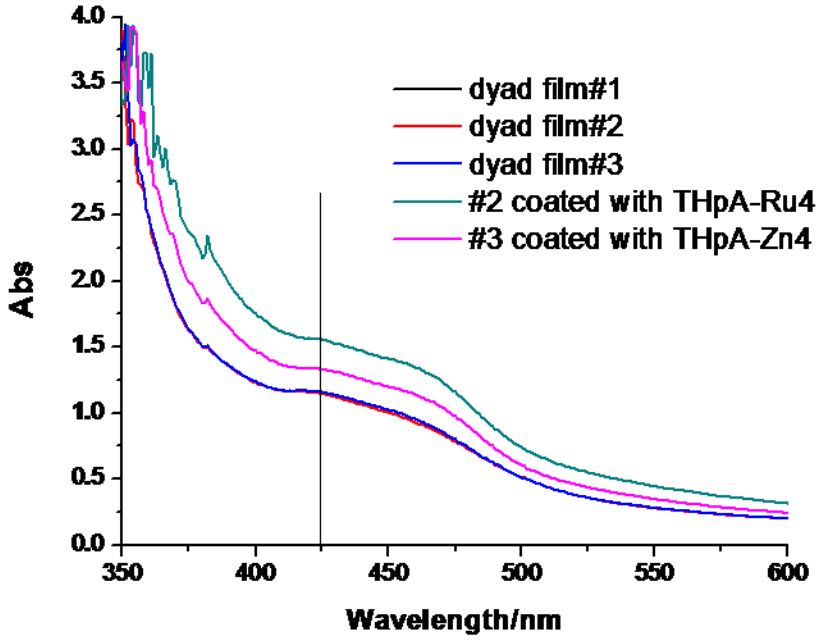

Figure 3.5 UV-Vis spectra of the dyad film (black), triad films with THpA-Ru_4POM (cyanine-green) and the control triad film with THpA-Zn_4POM (magenta). All measurements were referenced to air.

3.2 Electrodes with C2P2 as Sensitizer

3.2.1 UV-Vis Spectra and Stability

In theory, comparison of the stability of electrodes with P2 as the sensitizer and the ones with C2P2 as the sensitizer is far from accurate because preparation of the C2P2 electrodes involves further soaking in salt solutions which aren't involved in preparation of the P2 electrodes. Different procedures make it hard to identify key factors affecting stability or to rule out variables that have little impact. Here a rough comparison was made based on the loss of absorbance (percentage calculated, the smaller number was calculated without subtracting the TiO_2 absorbance while the larger number involves subtraction of the TiO_2 absorbance) after PEC experiments for three electrodes: 1) with P2 sensitizer; 2) with C2P2 sensitizer but not soaked in Na^+ solution before catalyst immobilization; and 3) with C2P2 as sensitizer with subsequent incorporation of Na^+ (by soaking the electrode in NaCl solution prior to catalyst immobilization).

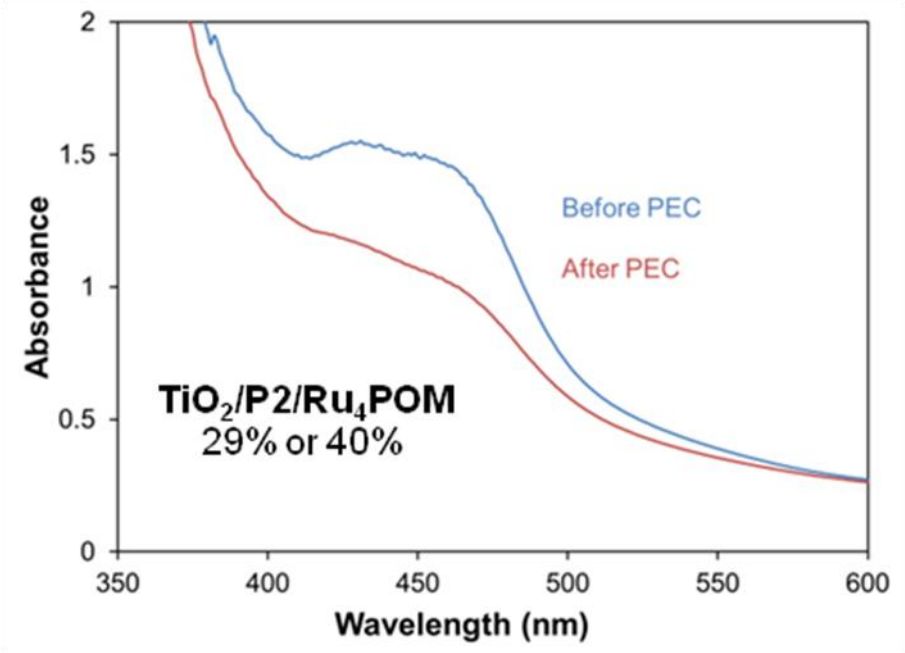

Figure 3.6 UV-Vis spectra of the dry P2-based triad electrode before/after use as a PEC. The calculated percentage of dye during the PEC experiment is evident.

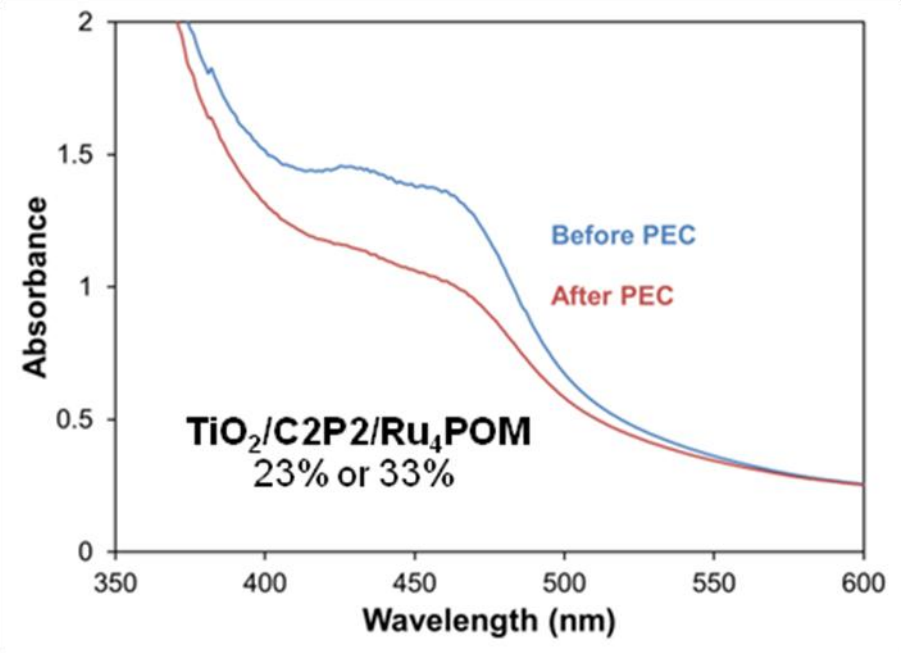

Figure 3.7 UV-Vis spectra of the dry C2P2-based electrode before/after uses a PEC.

The calculated percentage of dye loss during the PEC experiment is smaller

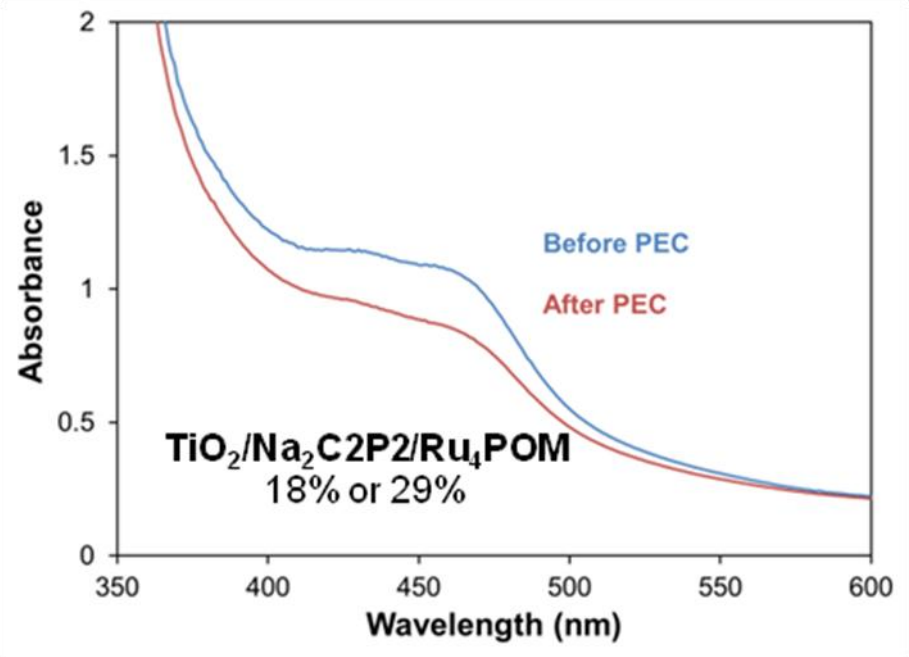

Figure 3.8 UV-Vis spectra of the dry Na_2C2P2-based electrode before/after uses a PEC. The calculated percentage of dye loss is even smaller.

From the percentage of dye lost, it is reasonable to conclude that C2P2 is more stable on the electrode, very likely due to its ability to capture cations in the crown ether groups. Sensitizer molecules with higher positive charges should be more strongly attracted to the highly negatively-charged POM catalyst.

3.2.2 Photoelectrochemical Measurements

When the P2 dye was replaced by C2P2, which was supposedly a more stable version of the well-known P2, photoelectrochemical measurements gave more complicated results.

As shown in Figure 3.9, when the same 500 mV external bias is applied to the system, the triad electrodes actually show a lower photocurrent enhancement compared to the dyad electrode and the C2P2 with crown-ether-bound Na^+ show poorer results than C2P2 with crown-ether-bound Li^+.

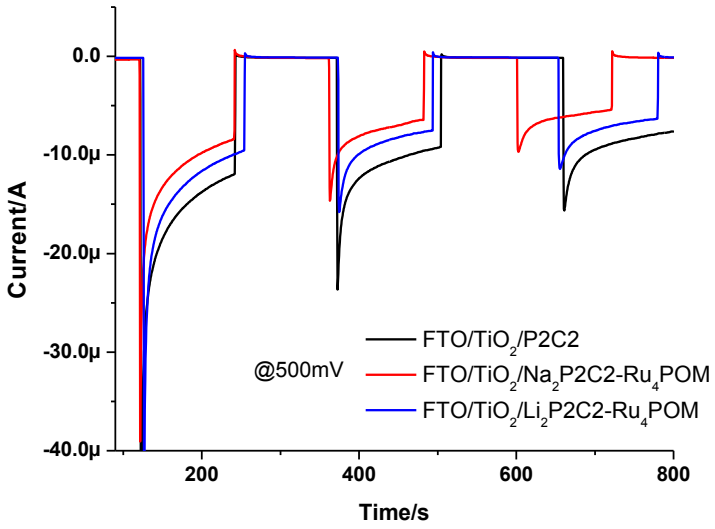

Figure 3.9 Single-potential time-based results for the dyad (black), the triad with crown-ether-bound Na^+ in C2P2 (red) and the triad with crown-ether-bound Li^+ in C2P2 (blue) with an applied bias of 500 mV.

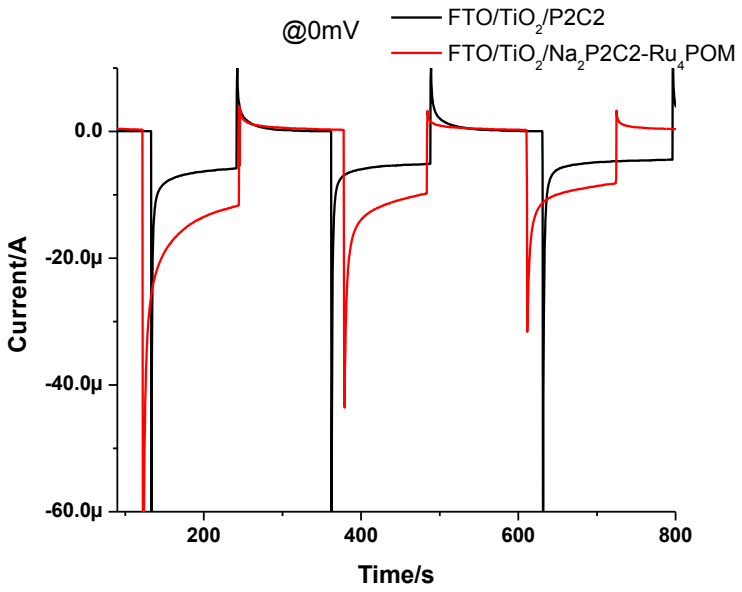

Figure 3.10 Single-potential time-based results for the dyad (black), triad with crown-ether-bound Na^+ as cation in C2P2 (red) with applied bias of 0mV.

This seemingly abnormal decrease in photocurrent from dyad to triad is explained by the computational data (see Figure 3.11 below) addressing the energetics of C2P2 in its ground state and excited states.

For P2 and Na_2C2P2, the HOMOs of the ground singlet electronic states involve the Ru-based orbitals. For C2P2 the HOMO is based on the 5-crown-phen ligand with the Ru-based HOMO being 0.34 eV lower in energy. The LUMOs are located on the bpy ligands in P2 and unmetallated C2P2. Interestingly, coordination of Na^+ moves the LUMO of C2P2 to the 5-crown-phen ligands. The LUMO corresponding to the bpy(phosphonate) ligand is another 0.43eV higher in energy. Therefore the MLCT transition in metallated C2P2 corresponds to the Ru-to-5-crown-phen transition, rather than the Ru-to-bpy(phosphonate) transition as seen in P2. It is quite reasonable that this would impede the desired electron transfer to TiO_2.

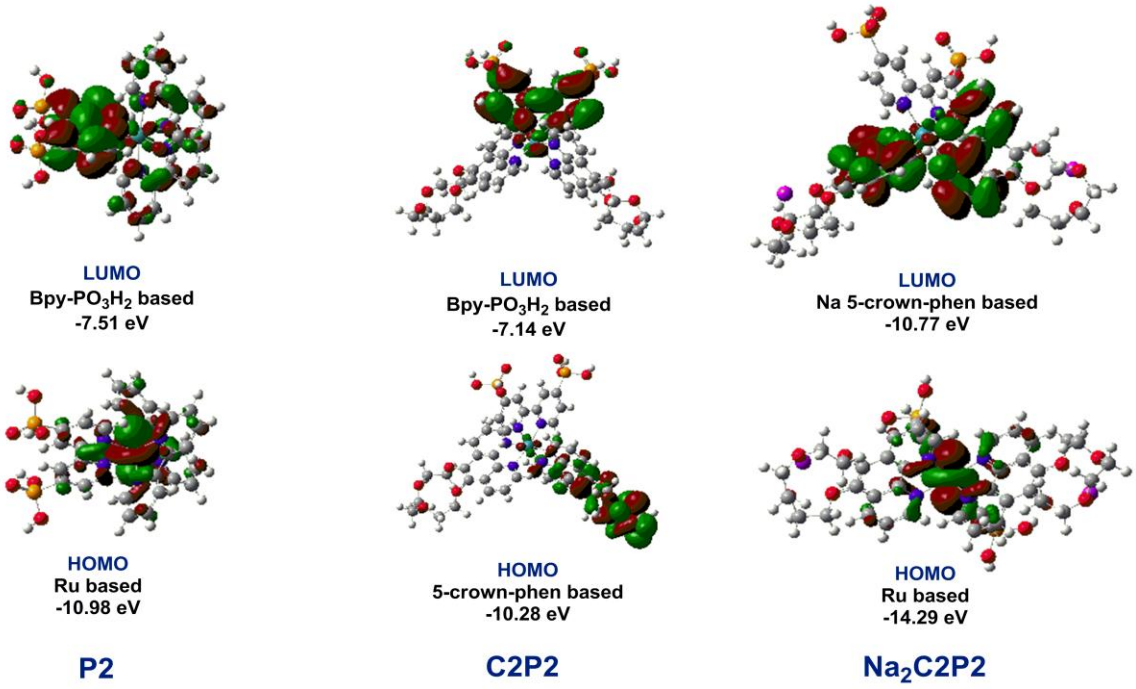

Figure 3.11 The calculated electronic structures and energies of the frontier orbitals of P2, C2P2 and metallated Na_2C2P2. DFT/B3LYP calculations by Dr. Djamaladdin G. Musaev.

(Courtesy of Dr. Djamaladdin G. Musaev)

Chapter 4:

Summary

This work presents an experimental study of immobilizing a known homogeneous WOC onto a dye-sensitized TiO_2 electrode and some preliminary results on potentials and dynamics. To date, most WOCs immobilized on electrode surfaces are metal nanoparticles, metal oxides clusters. In the systems investigated in this thesis, homogeneous WOCs are readily displaced, likely by buffer molecules, from the electrode surfaces when immersed in aqueous buffer solutions.

We have reported a successful method for immobilizing the homogeneous polyoxometalate WOC, Ru_4POM. The water-soluble POM is first converted to a highly hydrophobic and thus much less water-soluble derivative, by replacing its inorganic cation, typically Na^+, with tetraheptyl ammonium cation. This dye-modified TiO_2 electrode can then be soaked in a toluene solution of the POM resulting in rapid POM surface immobilization by electrostatic and or physisorption processes. THpA cations form a hydrophobic surface protecting the POM anions from displacement from the electrode surface. Such triad electrodes are reasonably stable.

We also compared the effects of two different sensitizers, P2 and C2P2 on the photocurrents. Single-potential time-based measurements show that P2-sensitized TiO_2 functionalized by Ru_4POM under an applied bias of 500mV and C2P2-sensitized TiO_2 functionalized by Ru_4POM under 0 mV of applied bias exhibit observable photocurrent enhancement compared with the dye-modified electrodes without water oxidation catalysts (the dyads). For the C2P2 photosensitizer, the effects of crown-ether-bound cations (e.g. Na^+, Li^+) on the electron injection kinetics were noted. The presence of Na^+ improves electron injection into the conduction band of TiO_2 in the TiO_2-PS-Na_2C2P2 triad assembly after visible excitation. That is, electron transfer

from the excited states of the PS (dye) into the WOC could be effectively suppressed, which is favorable for enhancement of the catalytic performance in the photogenerated hole-promoted water oxidation reactions. In addition, the experimental results are in good agreement with computational data on energetics of the components of the electrodes (the frontiers orbitals and their energies in the different dyes).

However, detection of oxygen has not been observed from bulk electrolysis on the electrodes. This is a consequence of the fact that the electrode surface area is too small for a detectable (by an oxygen probe) amount of oxygen gas to be produced.

In conclusion, triad electrodes can be optimized by adjusting the energetics of the components, studying the interface between electrolyte and electrode and using more stable sensitizers and faster water oxidation catalysts. This work defines a potential route for constructing efficient photoanodes comprising a semiconductor substrate, a photo-sensitizer and a molecular water oxidation catalyst.

References

1. Grätzel, M., *Solar Energy Conversion by Dye-Sensitized Photovoltaic Cells.* Inorganic Chemistry, 2005. **44**(20): p. 6841-6851.

2. Wiorkowski, J.J., *Estimating Volumes of Remaining Fossil Fuel Resources: A Critical Review.* Journal of the American Statistical Association, 1981. **76**(375): p. 534-548.

3. Hagfeldt, A. and M. Grätzel, *Molecular Photovoltaics.* Accounts of Chemical Research, 2000. **33**(5): p. 269-277.

4. Gratzel, M., *Photoelectrochemical cells.* Nature, 2001. **414**(6861): p. 338-344.

5. O'Regan, B. and M. Gratzel, *A low-cost, high-efficiency solar cell based on dye-sensitized colloidal TiO_2 films.* Nature, 1991. **353**(6346): p. 737-740.

6. Poudyal, K.N., et al., *Study of Global Solar Radiation Potential and Ground Level Albedo at Benevento Italy*. 2011. Vol. 8. 2011.

7. Lewis, N.S. and D.G. Nocera, *Powering the planet: Chemical challenges in solar energy utilization.* Proceedings of the National Academy of Sciences, 2006. **103**(43): p. 15729-15735.

8. Blankenship, R.E., et al., *Comparing Photosynthetic and Photovoltaic Efficiencies and Recognizing the Potential for Improvement.* Science, 2011. **332**(6031): p. 805-809.

9. Parkinson, B.A., A. Heller, and B. Miller, *Enhanced photoelectrochemical solar-energy conversion by gallium arsenide surface modification.* Applied Physics Letters, 1978. **33**(6): p. 521-523.

10. Balzani, V., et al., *Solar Energy Conversion by Water Photodissociation.* Science, 1975. **189**(4206): p. 852-856.

11. Nozik, A.J., *Photoelectrochemistry: Applications to Solar Energy Conversion.* Annual Review of Physical Chemistry, 1978. **29**(1): p. 189-222.

12. Wagner, S., *Photovoltaic Solar Cells,* in *Solid State Chemistry of Energy Conversion and Storage*. 1977, AMERICAN CHEMICAL SOCIETY. p. 109-133.

13. Copeland, A.W., O.D. Black, and A.B. Garrett, *The Photovoltaic Effect.* Chemical Reviews, 1942. **31**(1): p. 177-226.

14. Walter, M.G., et al., *Solar Water Splitting Cells.* Chemical Reviews, 2010. **110**(11): p. 6446-6473.

15. Youngblood, W.J., et al., *Photoassisted Overall Water Splitting in a Visible Light-Absorbing Dye-Sensitized Photoelectrochemical Cell.* Journal of the American Chemical Society, 2009. **131**(3): p. 926-927.

16. Yamazaki, H., et al., *Electrocatalytic and photocatalytic water oxidation to dioxygen based on metal complexes.* Coordination Chemistry Reviews, 2010. **254**(21-22): p. 2483-2491.

17. Lanz, M., D. Schürch, and G. Calzaferri, *Photocatalytic oxidation of water to O2 on AgCl-coated electrodes.* Journal of Photochemistry and Photobiology A: Chemistry, 1999. **120**(2): p. 105-117.

18. Grätzel, M., *Dye-sensitized solar cells.* Journal of Photochemistry and Photobiology C: Photochemistry Reviews, 2003. **4**(2): p. 145-153.

19. Abe, R., *Recent progress on photocatalytic and photoelectrochemical water splitting under visible light irradiation.* Journal of Photochemistry and Photobiology C: Photochemistry Reviews, 2010. **11**(4): p. 179-209.

20. Hagfeldt, A., et al., *Dye-Sensitized Solar Cells.* Chemical Reviews, 2010. **110**(11): p. 6595-6663.

21. Inoue, T., et al., *Photoelectrocatalytic reduction of carbon dioxide in aqueous suspensions of semiconductor powders.* Nature, 1979. **277**(5698): p. 637-638.

22. Maruska, H.P. and A.K. Ghosh, *Photocatalytic decomposition of water at semiconductor electrodes.* Solar Energy, 1978. **20**(6): p. 443-458.

23. Livraghi, S., et al., *Preparation and spectroscopic characterization of visible light sensitized N doped TiO_2 (rutile).* Journal of Solid State Chemistry, 2009. **182**(1): p. 160-164.

24. Kim, Y., et al., *Enhanced Performance of Dye-Sensitized TiO_2 Solar Cells Incorporating COOH-Functionalized Si Nanoparticles.* Chemistry of Materials, 2009. **22**(1): p. 207-211.

25. Nozik, A.J., *Quantum dot solar cells.* Physica E: Low-dimensional Systems and Nanostructures, 2002. **14**(1–2): p. 115-120.

26. Chen, M., et al., *Star-Shaped Light-Harvesting Polymers Incorporating an Energy Cascade.* Angewandte Chemie International Edition, 2005. **44**(28): p. 4368-4372.

27. Dürr, H. and S. Bossmann, *Ruthenium Polypyridine Complexes. On the Route to Biomimetic Assemblies as Models for the Photosynthetic Reaction Center.* Accounts of Chemical Research, 2001. **34**(11): p. 905-917.

28. Thanasekaran, P., et al., *Marcus Inverted Region in the Photoinduced Electron Transfer Reactions of Ruthenium(II)−Polypyridine Complexes with Phenolate Ions.* The Journal of Physical Chemistry A, 1997. **101**(44): p. 8195-8199.

29. Rajagopal, S., et al., *Excited state electron transfer reactions of tris(4,4'-dialkyl-2,2'-bipyridine)ruthenium(II) complexes with phenolate ions: structural and solvent effects.* Journal of Photochemistry and Photobiology A: Chemistry, 1992. **69**(1): p. 83-89.

30. Potvin, P.G., P.U. Luyen, and J. Bräckow, *Electrostatic Bubbles and Supramolecular Assistance of Photosensitization by Carboxylated Ru(II) Complexes.* Journal of the American Chemical Society, 2003. **125**(16): p. 4894-4906.

31. Gillaizeau-Gauthier, I., et al., *Phosphonate-Based Bipyridine Dyes for Stable Photovoltaic Devices.* Inorganic Chemistry, 2001. **40**(23): p. 6073-6079.

32. Montalti, M., et al., *Luminescent Ruthenium(II) Bipyridyl−Phosphonic Acid Complexes: pH Dependent Photophysical Behavior and Quenching with Divalent Metal Ions.* Inorganic Chemistry, 1999. **39**(1): p. 76-84.

33. Chen, J., et al., *Theoretical studies on spectroscopic properties of ruthenium sensitizers absorbed to TiO_2 film surface with connection mode for DSSC.* Dyes and Pigments, 2012. **94**(3): p. 459-468.

34. Gao, X.-Q., et al., *Structures and spectroscopic properties of ruthenium phenanthroline solar-cell sensitizers: A computational study.* Chemical Physics Letters, 2011. **506**(4–6): p. 146-151.

35. Li, L., et al., *A photoelectrochemical device for visible light driven water splitting by a molecular ruthenium catalyst assembled on dye-sensitized nanostructured TiO_2.* Chemical Communications, 2010. **46**(39): p. 7307-7309.

36. Yin, Q., et al., *A Fast Soluble Carbon-Free Molecular Water Oxidation Catalyst Based on Abundant Metals.* Science, 2010. **328**(5976): p. 342-345.

37. Luo, Z., et al., *Synthesis, Structure, and Magnetism of a Polyoxometalate with Coordinatively Unsaturated d-Electron-Transition Metal Centers.* Inorganic Chemistry, 2009. **48**(16): p. 7812-7817.

38. Kuznetsov, A.E., et al., *Dioxygen and Water Activation Processes on Multi-Ru-Substituted Polyoxometalates: Comparison with the "Blue-Dimer" Water Oxidation Catalyst.* Journal of the American Chemical Society, 2009. **131**(19): p. 6844-6854.

39. Huang, Z., et al., *Efficient Light-Driven Carbon-Free Cobalt-Based Molecular Catalyst for Water Oxidation.* Journal of the American Chemical Society, 2011. **133**(7): p. 2068-2071.

40. Geletii, Y.V., et al., *Polyoxometalates in the Design of Effective and Tunable Water Oxidation Catalysts.* Israel Journal of Chemistry, 2011. **51**(2): p. 238-246.

41. Geletii, Y.V., et al., *Structural, Physicochemical, and Reactivity Properties of an All-Inorganic, Highly Active Tetraruthenium*

Homogeneous Catalyst for Water Oxidation. Journal of the American Chemical Society, 2009. **131**(47): p. 17360-17370.

42. Harriman, A., et al., *Metal oxides as heterogeneous catalysts for oxygen evolution under photochemical conditions.* Journal of the Chemical Society, Faraday Transactions 1: Physical Chemistry in Condensed Phases, 1988. **84**(8): p. 2795-2806.

43. Morris, N.D. and T.E. Mallouk, *A High-Throughput Optical Screening Method for the Optimization of Colloidal Water Oxidation Catalysts.* Journal of the American Chemical Society, 2002. **124**(37): p. 11114-11121.

44. Morris, N.D., M. Suzuki, and T.E. Mallouk, *Kinetics of Electron Transfer and Oxygen Evolution in the Reaction of $[Ru(bpy)_3]^{3+}$ with Colloidal Iridium Oxide.* The Journal of Physical Chemistry A, 2004. **108**(42): p. 9115-9119.

45. Morris, W., et al., J. Am. Chem. Soc., 2010. **132**: p. 11006.

46. Kanan, M.W. and D.G. Nocera, *In Situ Formation of an Oxygen-Evolving Catalyst in Neutral Water Containing Phosphate and Co^{2+}.* Science, 2008. **321**(5892): p. 1072-1075.

47. Kanan, M.W., Y. Surendranath, and D.G. Nocera, *Cobalt-phosphate oxygen-evolving compound.* Chemical Society Reviews, 2009. **38**(1): p. 109-114.

48. Jiao, F. and H. Frei, *Nanostructured Cobalt Oxide Clusters in Mesoporous Silica as Efficient Oxygen-Evolving Catalysts.* Angewandte Chemie International Edition, 2009. **48**(10): p. 1841-1844.

49. Li, G., et al., *Deposition of an oxomanganese water oxidation catalyst on TiO_2 nanoparticles: computational modeling, assembly and characterization.* Energy & Environmental Science, 2009. **2**(2): p. 230-238.

50. Robinson, D.M., et al., *Water Oxidation by λ-MnO_2: Catalysis by the Cubical Mn_4O_4 Subcluster Obtained by Delithiation of Spinel LiMn2O4.* Journal of the American Chemical Society, 2010. **132**(33): p. 11467-11469.

51. Gorlin, Y. and T.F. Jaramillo, *A Bifunctional Nonprecious Metal Catalyst for Oxygen Reduction and Water Oxidation.* Journal of the American Chemical Society, 2010. **132**(39): p. 13612-13614.

52. Shevchenko, D., et al., *Photochemical water oxidation with visible light using a cobalt containing catalyst.* Energy & Environmental Science, 2011. **4**(4): p. 1284-1287.

53. Gersten, S.W., G.J. Samuels, and T.J. Meyer, *Catalytic oxidation of water by an oxo-bridged ruthenium dimer.* Journal of the American Chemical Society, 1982. **104**(14): p. 4029-4030.

54. Hurst, J.K., J. Zhou, and Y. Lei, *Pathways for water oxidation catalyzed by the (.mu.-oxo)bis[aquabis(bipyridine)ruthenium](4+) ion.* Inorganic Chemistry, 1992. **31**(6): p. 1010-1017.

55. Wada, T., K. Tsuge, and K. Tanaka, *Electrochemical Oxidation of Water to Dioxygen Catalyzed by the Oxidized Form of the Bis(ruthenium – hydroxo) Complex in H_2O.* Angewandte Chemie International Edition, 2000. **39**(8): p. 1479-1482.

56. Yagi, M., et al., *Molecular catalysts for water oxidation toward artificial photosynthesis.* Photochemical & Photobiological Sciences, 2009. **8**(2): p. 139-147.

57. Hurst, J.K., *Water oxidation catalyzed by dimeric μ-oxo bridged ruthenium diimine complexes.* Coordination Chemistry Reviews, 2005. **249**(3–4): p. 313-328.

58. Zong, R. and R.P. Thummel, *A New Family of Ru Complexes for Water Oxidation.* Journal of the American Chemical Society, 2005. **127**(37): p. 12802-12803.

59. Muckerman, J.T., et al., *Water Oxidation by a Ruthenium Complex with Noninnocent Quinone Ligands: Possible Formation of an O−O Bond at a Low Oxidation State of the Metal.* Inorganic Chemistry, 2008. **47**(6): p. 1787-1802.

60. Concepcion, J.J., et al., *One Site is Enough. Catalytic Water Oxidation by $[Ru(tpy)(bpm)(OH_2)]^{2+}$ and $[Ru(tpy)(bpz)(OH_2)]^{2+}$*. Journal of the American Chemical Society, 2008. **130**(49): p. 16462-16463.

61. Betley, T.A., et al., *A ligand field chemistry of oxygen generation by the oxygen-evolving complex and synthetic active sites.* Philosophical Transactions of the Royal Society B: Biological Sciences, 2008. **363**(1494): p. 1293-1303.

62. McDaniel, N.D., et al., *Cyclometalated Iridium(III) Aquo Complexes: Efficient and Tunable Catalysts for the Homogeneous Oxidation of Water.* Journal of the American Chemical Society, 2007. **130**(1): p. 210-217.

63. Brimblecombe, R., et al., *Sustained Water Oxidation Photocatalysis by a Bioinspired Manganese Cluster.* Angewandte Chemie International Edition, 2008. **47**(38): p. 7335-7338.

64. Romain, S., L. Vigara, and A. Llobet, *Oxygen−Oxygen Bond Formation Pathways Promoted by Ruthenium Complexes.* Accounts of Chemical Research, 2009. **42**(12): p. 1944-1953.

65. Hull, J.F., et al., *Highly Active and Robust Cp* Iridium Complexes for Catalytic Water Oxidation.* Journal of the American Chemical Society, 2009. **131**(25): p. 8730-8731.

66. Nishiwaki, N., et al., *Hydroxylated surface of GaAs as a scaffold for a heterogeneous Pd catalyst.* Physical Chemistry Chemical Physics, 2012. **14**(4): p. 1424-1430.

67. Dong, Y., et al., *Decoloration of three azo dyes in water by photocatalysis of Fe (III)–oxalate complexes/H_2O_2 in the presence of inorganic salts.* Dyes and Pigments, 2007. **73**(2): p. 261-268.

68. Tran, P.D., et al., *Recent advances in hybrid photocatalysts for solar fuel production.* Energy & Environmental Science, 2012. **5**(3): p. 5902-5918.

69. Long, D.-L., R. Tsunashima, and L. Cronin, *Polyoxometalates: Building Blocks for Functional Nanoscale Systems.* Angewandte Chemie International Edition, 2010. **49**(10): p. 1736-1758.

70. Long, D.-L., E. Burkholder, and L. Cronin, *Polyoxometalate clusters, nanostructures and materials: From self assembly to designer materials and devices.* Chemical Society Reviews, 2007. **36**(1): p. 105-121.

71. Geletii, Y.V., et al., *Homogeneous Light-Driven Water Oxidation Catalyzed by a Tetraruthenium Complex with All Inorganic Ligands.* Journal of the American Chemical Society, 2009. **131**(22): p. 7522-7523.

72. Geletii, Y.V., et al., *An All-Inorganic, Stable, and Highly Active Tetraruthenium Homogeneous Catalyst for Water Oxidation.* Angewandte Chemie International Edition, 2008. **47**(21): p. 3896-3899.

73. Zaban, A., A. Meier, and B.A. Gregg, *Electric Potential Distribution and Short-Range Screening in Nanoporous TiO_2 Electrodes.* The Journal of Physical Chemistry B, 1997. **101**(40): p. 7985-7990.

74. Longo, C., J. Freitas, and M.-A. De Paoli, *Performance and stability of TiO_2/dye solar cells assembled with flexible electrodes and a polymer electrolyte.* Journal of Photochemistry and Photobiology A: Chemistry, 2003. **159**(1): p. 33-39.

75. Katsoulis, D.E. and M.T. Pope, *New chemistry for heteropolyanions in anhydrous nonpolar solvents. Coordinative unsaturation of surface atoms. Polyanion oxygen carriers.* Journal of the American Chemical Society, 1984. **106**(9): p. 2737-2738.